

# Tm<sup>3+</sup> waveguide lasers in monoclinic double tungstates

Western Bolaños Rodríguez

Física i Cristal·lografia de Materials i Nanomaterials (FiCMA-FiCNA). Department de Química Física i Inorgànica, Universitat Rovira i Virgili, C/Marcel·lí Domingo S/N, 43007, Tarragona, Spain

## 1. Abstract

CW waveguide laser oscillation at  $\sim 1.84 \mu\text{m}$  have been demonstrated in Tm-doped  $\text{KY}_{1-x-y}\text{Gd}_x\text{Lu}_y(\text{WO}_4)_2$  planar and channel waveguides. On one hand, buried planar waveguides were obtained by means of liquid phase epitaxy (LPE) of the active and cladding layers over  $\text{KY}(\text{WO}_4)_2$  substrates. On the other hand, buried channel waveguides were fabricated by a novel fabrication process that consists on the direct structuring of a  $\text{KY}(\text{WO}_4)_2$  substrate, followed by epitaxial lateral overgrowth (ELO) by LPE on these structured substrates, and finishing the process by growing an epitaxial cladding layer with the same composition of the substrate. In addition, using the buried planar waveguide, passive Q-switched lasing was also demonstrated. These results have been published in *Optics Express* vol. 18, No. 26, 26937-16945 (2010), *Optics Express* vol. 19, No.2, 1449-1454 (2011) and *Optical Materials Express* vol. 1, No. 3, 306-315 (2011).

## 2. Introduction

Monoclinic potassium double tungstates,  $\text{KRE}(\text{WO}_4)_2$  ( $\text{RE} = \text{Y}, \text{Gd}, \text{Lu}$ ) have emerged as excellent hosts for lasing ions, especially lanthanides, since they present very large absorption and emission cross-sections for the active ions, and because in their structure there is a relatively large ion separation allowing high doping levels with minimum concentration quenching effects. This, together with the relatively high refractive index values, made them interesting materials for the fabrication of compact integrated photonic devices [1].

Laser emission in the  $2 \mu\text{m}$  spectral range is of particular interest for applications in atmospheric monitoring, laser radar and medicine. This is mainly due to the strong absorption bands of water around this wavelength. Optical parametric oscillators (OPOs) operating in the mid-IR region also require  $2 \mu\text{m}$  lasers as pumping sources. Among the lanthanide ions exhibiting laser transitions around  $2 \mu\text{m}$ , the trivalent thulium ( $\text{Tm}^{3+}$ ) with the emission based on the  ${}^3\text{F}_4 \rightarrow {}^3\text{H}_6$  transition is one of the most attractive, since it can be pumped directly around  $800 \text{ nm}$  with AlGaAs diode lasers.

Waveguide lasers with their simple monolithic structure are attractive for integrated optical devices with the potential for on-chip integration. The inherent advantage of waveguide lasers over conventional bulk lasers is the good overlap between the pump light and the laser mode, because both are constrained to propagate together in the narrow waveguide, leading to high intensities for relatively low power. Furthermore, the waveguide laser geometry is in particular advantageous for three-level lasers in which the final level is thermally populated, such as  $\text{Tm}^{3+}$ .

There are only few reports about waveguide lasers based on  $\text{Tm}^{3+}$ , involving YAG [2], and  $\text{LiNbO}_3$  [3]. The only report on lasing of a Tm-doped monoclinic double tungstate planar waveguide structure was based on  $\text{Tm}:\text{KY}(\text{WO}_4)_2$ . However, the waveguide was placed in a  $\sim 1 \text{ m}$  long external cavity [4].

A summary of the results obtained on the development and characterization of  $\text{Tm}^{3+}$ -doped waveguide lasers on epitaxial layers of monoclinic potassium double tungstates is presented herein.

## 3. Description of the waveguides fabrication processes

### 3.1 Buried planar waveguides

Figure 1 presents the schematics of the fabrication process of buried planar waveguides. The guiding layer  $\text{KY}_{0.57}\text{Gd}_{0.22}\text{Lu}_{0.17}\text{Tm}_{0.03}(\text{WO}_4)_2$  was grown over the substrate by LPE. Then one of the large faces of the substrate is removed and the other one was polished down to a thickness of  $12 \mu\text{m}$ . After

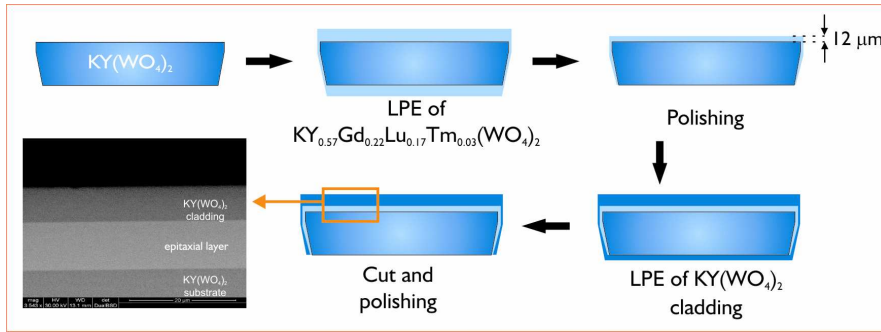


Figure 1. Buried planar waveguide fabrication process. The image on the left bottom shows the aspect of the end-faces after polishing them.

that, a top cladding layer of  $\text{KY}(\text{WO}_4)_2$  was overgrown over the polished active layer leading to a buried planar waveguide as can be seen in the cross-sectional ESEM image in figure 1.

### 3.2 Buried channel waveguides

I have developed and optimized a novel procedure for the fabrication of channel waveguides in dielectric materials by combining standard UV photolithography, Ar-ion milling and LPE. A summary of that novel procedure can be seen in figure 2.

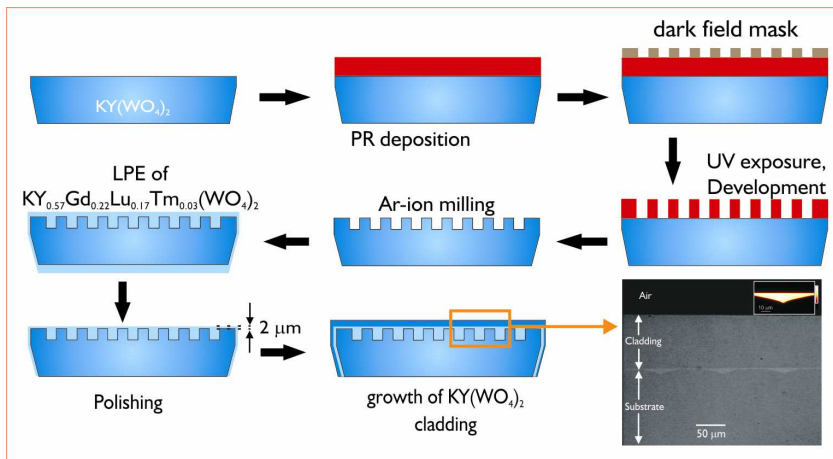


Figure 2. Buried channel waveguide fabrication process. The image on the right bottom shows the cross-view of some representative channels with trapezoidal shape. The inset in such image shows the  $\text{Tm}^{3+}$  luminescence map taken with a confocal microscope. Despite the trapezoidal shape, highly confined light was observed at different wavelengths.

The microfabrication process can be summarized as follows: (i) Microstructuring of a  $\text{KY}(\text{WO}_4)_2$  substrate by UV photolithography and Ar-ion milling. (ii) Epitaxial Lateral Overgrowth (ELO) of the Tm-doped  $\text{KY}_{1-x-y}\text{Gd}_x\text{Lu}_y(\text{WO}_4)_2$  lattice matched layer over the surface of the microstructured  $\text{KY}(\text{WO}_4)_2$  substrate. (iii) LPE growth of a  $\text{KY}(\text{WO}_4)_2$  cladding layer. This method included one main difference when compared to previous methods used for the fabrication of buried channel waveguides and it is the direct structuring of the substrate, followed by a regrowth of the active layer on these structured substrates, and finishing the process by growing a cladding layer with the same composition of the substrate.

### 4. Waveguide laser setup and results

Waveguide laser experiments were performed by using an argon-ion-pumped Ti:Sapphire laser operating at 802 nm. The pump signal was coupled into the waveguide by means of a  $10\times$  long working distance microscope objective lens ( $\text{NA} = 0.28$ ). The sample was placed on a tilt stage mounted on a precision XYZ stage. The output signal coming from the waveguide was collected by means of a  $50\times$  objective lens ( $\text{NA} = 0.42$ ) and then focused onto a laser spectrometer as can be seen in figure 3.

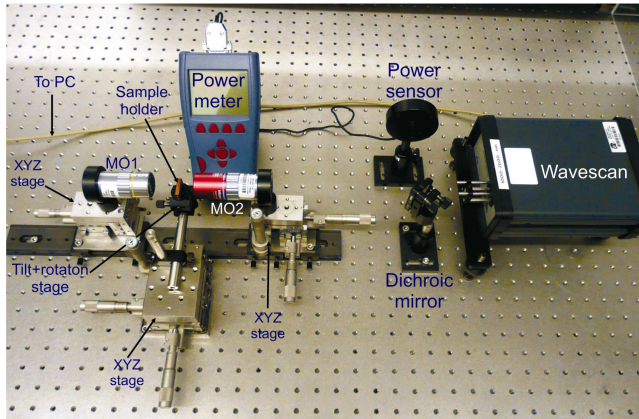


Figure 3. Laser cavity experimental setup. MO: Microscope objective. The dichroic mirror, placed at 45°, between the MO2 and the laser spectrometer (wavescan) was used to reflect the laser emission at 1.84  $\mu\text{m}$  from the waveguide onto the power sensor, allowing the transmitted pump signal to cross through the dichroic mirror.

#### 4.1 CW planar waveguide laser [5]

Planar waveguide lasing was demonstrated in a monolithic cavity in the 2  $\mu\text{m}$  spectral range. This laser was operating in the continuous wave regime and in the Q-switch mode using a Cr:ZnSe crystal as saturable absorber (SA). The laser cavity was formed by butting two dielectric mirrors against the ends of the sample. These mirrors were held in place by the surface tension of a film index matching gel. The input coupler mirror had a dichroic coating with high transmission (93%) at 802 nm and high reflection (99%) at 1800 nm, whilst the transmission of the output coupler at the laser wavelength was 0.2%.

The absorbed power to reach the laser threshold was only 40 mW. At maximum absorbed pump power of 66 mW, the output power reached 5.5 mW, leading to an optical efficiency of 8.3%. The slope efficiency obtained with respect to the absorbed pump power amounted to 23%. The planar waveguide laser emitted at a wavelength of 1843.6 nm. The laser output was found to be linearly polarized, selected parallel to the  $N_m$  optical direction. From the near field distribution of the laser mode, the waist size (full-width at 1/e) was calculated to be 5  $\mu\text{m}$  in the vertical direction.

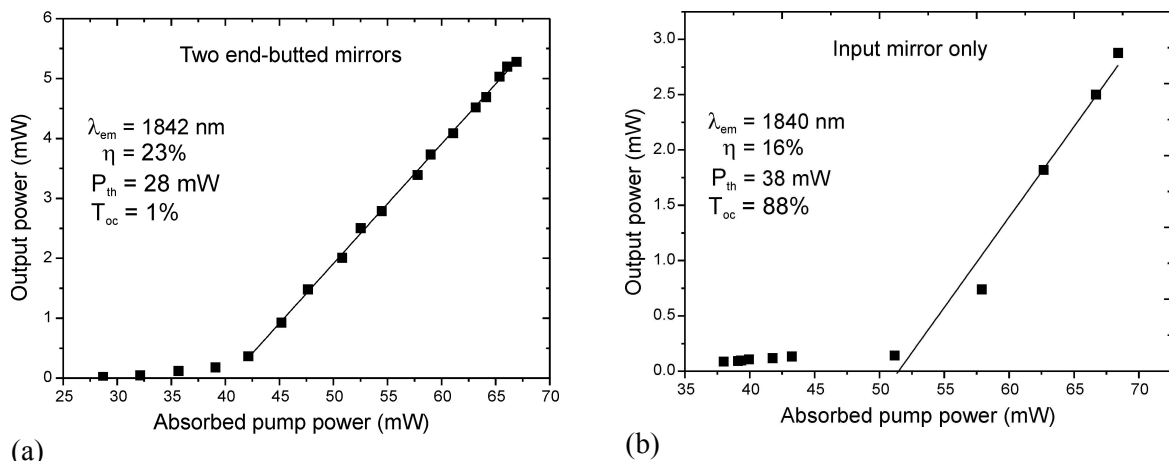


Fig. 4. Laser operation for the TE pump polarization using (a) two dielectric mirrors and (b) the input mirror only.

CW laser oscillation could also be observed even when the output mirror was removed from the waveguide end face. The Fresnel reflection of the output end face led to a transmission of 88% which produced a drop of the slope efficiency from 23% (when 1% transmission output coupler was used) to 16%. The laser threshold was increased to around 50 mW and the laser delivered  $\sim 3$  mW at a maximum absorbed pump power of 66 mW. The laser characteristics of the  $\text{KY}_{0.58}\text{Gd}_{0.22}\text{Lu}_{0.17}\text{Tm}_{0.03}(\text{WO}_4)_2$  planar waveguide using the two dielectric mirrors and the input mirror only are shown in Figure 4.

## 4.2 Q-switch planar waveguide laser [5]

This  $\text{KY}_{0.58}\text{Gd}_{0.22}\text{Lu}_{0.17}\text{Tm}_{0.03}(\text{WO}_4)_2$  planar waveguide laser operating in the CW regime was used for the realization of the first ever Tm doped pulsed waveguide laser

. This was achieved by introducing into the cavity a 0.89 mm thick plate of Cr:ZnSe as saturable absorber (SA). In this way, passively Q-switched operation was demonstrated. The SA crystal was butt-coupled between the output coupler and the end face of the planar waveguide, as can be seen in Figure 5.

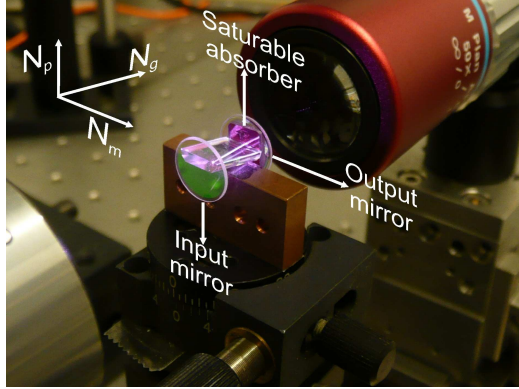


Fig. 5. Planar waveguide laser setup formed with the SA at the output.

separating the end mirror from the waveguide by nearly 1 mm when placing the SA. The pulse repetition frequency was found to be increased almost linearly from 4 kHz at the highest pump level.

The passive Q-switch laser was reached at an absorbed pump power of 41 mW. The output spectrum consisted of a single peak centered at 1844.7 nm and exhibited a spectral linewidth  $< 0.5$  nm. At the highest absorbed pump power of 66 mW, the total average output power reached 1.2 mW. The optical conversion efficiency with respect to the absorbed pump power was 1.8%.

The average output power characteristics showed a nearly linear dependence corresponding to a slope efficiency of 5%. The reduction of the slope efficiency compared with the CW case is due to the additional losses introduced into the cavity when

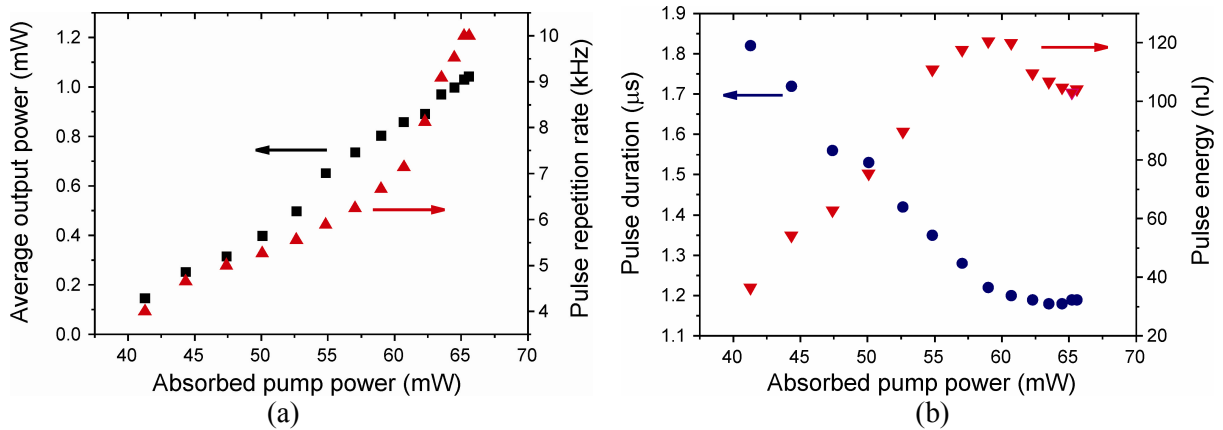


Figure 6. Operation performance of the Q-switch planar waveguide laser . (a) Average output power and pulse repetition rate as a function of the absorbed pump power. (b) Pulse duration and calculated pulse energy as a function of the absorbed pump power.

The maximum pulse energy was estimated to be 120 nJ at a pulse repetition frequency of 7 kHz. The pulse duration decreased from 1.8  $\mu\text{s}$  (FWHM) at threshold asymptotic to 1.2  $\mu\text{s}$  for maximum absorbed pump power. Figure 6 shows the laser characteristics of the Q-switch planar waveguide laser achieved. By single pass transmission measurements at  $\lambda = 632.8$  nm, we established that the upper limit for optical losses was 0.4 dB/cm assuming 100% of coupling efficiency between the pump and the guided modes.

## 4.3 CW channel waveguide laser [6, 7]

The very first demonstration of CW lasing with the  $\text{KY}_{0.58}\text{Gd}_{0.22}\text{Lu}_{0.17}\text{Tm}_{0.03}(\text{WO}_4)_2$  buried channel waveguides was carried out using the waveguides fabricated as explained in section 3.

Laser operation of the transition  ${}^3\text{F}_4 \rightarrow {}^3\text{H}_6$  levels of  $\text{Tm}^{3+}$  in the continuous wave regime at room temperature was obtained in several buried channel waveguides. The feedback provided by the 11% Fresnel reflections at the end faces alone was sufficient to enable laser oscillation, allowing the

operation of a mirrorless guided laser for the TE and TM pump polarizations. Laser characteristic corresponding to the TE and TM pump polarizations are presented in Figure 7.

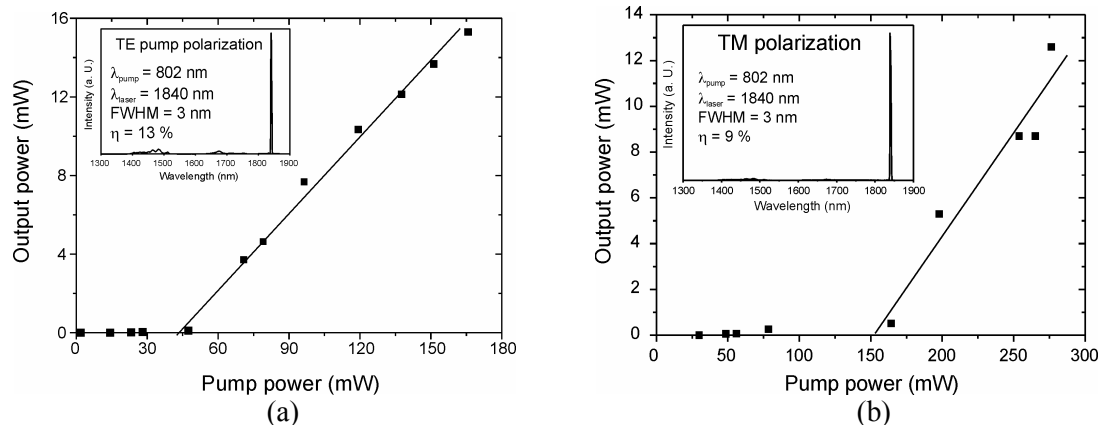


Figure 7.  $KY_{0.58}Gd_{0.22}Lu_{0.17}Tm_{0.03}(WO_4)_2$  buried channel waveguide laser characteristics for (a) TE and (b) TM pump polarizations.

The emission wavelength was  $1.84 \mu\text{m}$  for both polarizations. For the TE pump polarization, a maximum output power of 15 mW was obtained for an incident pump power of 165 mW, whilst for the TM pump polarization, the maximum output power obtained was 5.5 mW for an incident pump power of 170 mW. Efficiencies of 13 % and 6 % with respect to the incident pump power for the TE and TM pump polarizations were obtained, respectively. Additionally, the power thresholds necessary for reaching the laser operation were found to be 50 mW and 60 mW for TE and TM pump polarizations, respectively. The upper limit for optical losses associated to this buried channel waveguides was estimated to be 0.2 dB/cm, that was evaluated by the single pass transmission method at  $\lambda = 632.8 \text{ nm}$

#### 4.4 References

- [1] M. Pollnau, Y. E. Romanyuk, F. Gardillou, C. N. Borca, U. Griebner, S. Rivier and V. Petrov, "Double tungstate lasers : from bulk toward on-chip integrated waveguide devices". IEEE J. Sel. Top. Quantum Electron. 13, 661-671 (2007).
- [2] J. I. Mackenzie, S. C. Mitchell, R. J. Beach, H. E. Meissner, and D. P. Shepherd, "15 W diode-side-pumped Tm:YAG waveguide laser at  $2 \mu\text{m}$ ", Electron. Lett. 37, 898-899 (2001).
- [3] Cantelar, J. A. Sanz-García, G. Lifante and F. Cussó, "Single polarizad  $Tm^{3+}$  laser in Zn-diffused  $LiNbO_3$  channel waveguides," Appl. Phys. Lett. 86, 161119-1-161119-3 (2005).
- [4] S. Rivier, X. Mateos, V. Petrov, U. Griebner, Y. E. Romanyuk, C. N. Borca, F. Gardillou, and M. Pollnau, "Tm:  $KY(WO_4)_2$  waveguide laser" Opt. Express 15, 5885-5892 (2007).
- [5] W. Bolaños, J.J. Carvajal, X. Mateos, E. Cantelar, G. Lifante, U. Griebner, V. Petrov, V.L. Panyutin, G.S. Murugan, J.S. Wilkinson, M. Aguiló, F. Díaz, "Continuous-wave and Q-switched Tm-doped  $KY(WO_4)_2$  planar waveguide laser at  $1.84 \mu\text{m}$ ", Opt. Express 19, 1449-1454 (2011).
- [6] W. Bolaños, J.J. Carvajal, X. Mateos, G.S. Murugan, A.Z. Subramanian, J.S. Wilkinson, E. Cantelar, D. Jaque, G. Lifante, M. Aguiló and F. Díaz, "Mirrorless buried waveguide laser in monoclinic double tungstates fabricated by a novel combination of ion milling and liquid phase epitaxy" Opt. Express 18, 26937-26945, (2010).
- [7] W. Bolaños, J. J. Carvajal, X. Mateos, G. Lifante, G. S. Murugan, J. S. Wilkinson, M. Aguiló and F. Díaz, "análisis of confinement effects on microstructured  $Ln^{3+}:KY_{1-x-y}Gd_xLu_y(WO_4)_2$  waveguides", Opt. Mat. Exp. 1, 306-315 (2011).